

Two inert scalar doublet model and $h \rightarrow \gamma\gamma, \gamma Z$ at LHC

E. C. F. S. Fortes,^{*} A. C. B. Machado,[†] J. Montaña,[‡] and V. Pleitez[§]

Instituto de Física Teórica–Universidade Estadual Paulista

R. Dr. Bento Teobaldo Ferraz 271, Barra Funda

São Paulo - SP, 01140-070, Brazil

(Dated: 10/08/14)

We consider the decays $h \rightarrow \gamma\gamma, \gamma Z$ in the context of a model with two inert Higgs doublets and an additional S_3 symmetry to the SM content. This model besides having good candidates for dark matter also has contributions for these latter processes through charged scalars-loops. We found that when considering the more precise available experimental data for $h \rightarrow \gamma\gamma$ and the correlation between both channels, the enhancement for $h \rightarrow \gamma Z$ can not be larger than 1.2 times the standard model prediction.

PACS numbers: 12.60.Fr, 14.80.Fd, 12.15.Ji

I. INTRODUCTION

The recent discovery at the LHC indicates, for the first time, that at least one fundamental neutral scalar, here denoted by h , does exist in nature. Moreover, all its properties that have been measured until now, are compatible with the predictions of the standard model (SM) Higgs boson. For instance, it is a spin-0 and CP even scalar [1, 2] and its couplings with gauge bosons and heavy fermions are compatible with those of the SM within the experimental error [3, 4]. Notwithstanding, the data do not rule out the existence of new physics, in particular, processes induced at loop level have always been important to seek such evidence. This is the case of the decays $h \rightarrow \gamma\gamma$ and $h \rightarrow \gamma Z$ because they may have contributions from new charged particles. Recently, ATLAS and CMS Collaborations have measured the decay ratios for both processes [5–8]. The decay in two photons is now closer to SM prediction, if compared to 2012 data, but the decay to γZ has not been observed yet, however, ATLAS and CMS have presented upper limits for this decay, see Table I.

Moreover, motivated by physics of the dark matter (DM), neutrinos masses, hierarchy problem, and any other physics beyond the SM, there are many phenomenological models that extend the scalar sector of the SM with one or more scalar multiplets. A simple extension of the SM consists in the addition of two extra scalar doublets to the SM particle content. In this case, if a discrete symmetry S_3 is assumed and with a particular vacuum alignment, the two extra scalar doublets are inert: all the SM particles are singlets under S_3 while the two new Higgs doublets form a S_3 doublet, so this new scalars interact only with the gauge bosons and with SM-like Higgs through trilinear and quartic terms [9]. We call this model IDMS₃ as in Ref. [10], where we shown that the model has DM candidates. The Higgs mechanism provides a portal for communication between the inert sector and the known particles.

In general, in multi-Higgs models, and in particular models with inert doublets, the Higgs production is the same as in the SM, however the decays $h \rightarrow \gamma\gamma$ and $h \rightarrow \gamma Z$ can receive corrections due to the contributions of charged scalars in loops. The phenomenology of IDM had been extensively discussed: i) in the context of DM phenomenology [11–17], ii) for collider phenomenology [18–20] and, iii) IDM has been also advocated to improve the naturalness idea [21, 22].

Analyzing the results presented in Table I, we note that the upper limit of the decay $h \rightarrow \gamma Z$ is one order of magnitude larger than its expected value in the SM ($R_{\gamma Z} = 1$). If this enhancement is confirmed in the future data, undoubtedly this will be a clear evidence for new physics. The ratios of $h \rightarrow \gamma\gamma$ and $h \rightarrow \gamma Z$ were analyzed in the context of the IDM in Refs. [23, 24] and in a general three Higgs doublet model in Ref. [25]. Here, we will extend this analysis to the context of the IDMS₃ using the recent data from ATLAS and CMS. We will show that it is not possible to expect an enhancement twice the SM prediction in the process $h \rightarrow \gamma Z$, even though there are two charged scalars in the model, but it is possible to have a small deviation lower than the SM prediction.

The outline of this paper is as follows. In Sec. II we briefly present the model of Ref. [9]. In Sec. III we calculate

^{*}Electronic address: elaine@ift.unesp.br

[†]Electronic address: ana@ift.unesp.br

[‡]Electronic address: montano@ift.unesp.br

[§]Electronic address: vicente@ift.unesp.br

the decays $h \rightarrow \gamma\gamma, \gamma Z$ in terms of the respective widths in SM. The results are shown in Sec. IV and the last section is designed for our conclusions. In the Appendix we give details about the form factors of the processes and their solutions in terms of the Passarino-Veltman scalar functions as well with their standard analytical solutions.

II. THE MODEL

Here we briefly discuss the model of Ref. [9], in which two of the SU(2) scalar doublets are inert because of the S_3 symmetry and a vacuum alignment. The three scalar doublets, given by $H_i = (\Phi_i^+ \Phi_i^0)^T$, are in the reducible triplet representation of S_3 , i.e. $\mathbf{3} = (H_1, H_2, H_3)$ and again this is broken down to the irreducible singlet and doublet ones, i.e., $\mathbf{3} = \mathbf{2} + \mathbf{1} \equiv D + S$, where:

$$S = \frac{1}{\sqrt{3}}(H_1 + H_2 + H_3) \sim \mathbf{1},$$

$$D \equiv (D_1, D_2) = \left[\frac{1}{\sqrt{6}}(2H_1 - H_2 - H_3), \frac{1}{\sqrt{2}}(H_2 - H_3) \right] \sim \mathbf{2}. \quad (1)$$

After the spontaneous symmetry breaking and due to the S_3 symmetry we can write the Higgs scalars doublet D and the singlet S in terms of the mass eigenstates as:

$$S \equiv \phi = \left(\frac{h^+}{\sqrt{2}}(3v + h^0 + iA^0) \right), \quad D \equiv -(\phi_1, \phi_2), \quad \phi_k = \left(\frac{h_k^+}{\sqrt{2}}(h_k^0 + iA_k^0) \right), \quad (2)$$

where $k = 2, 3$ and $h^0 \equiv h$ is the SM-Higgs.

In the case of CP-even, CP-odd neutral real scalars and for the charged ones, the masses are given by:

$$m_h^2 = 2\lambda_4 v_{SM}^2, \quad m_{h_2}^2 = m_{h_3}^2 \equiv m_H^2 = \mu_d^2 + \frac{1}{2}\lambda' v_{SM}^2, \quad (3)$$

$$m_{A_1}^2 = 0, \quad m_{A_2}^2 = m_{A_3}^2 \equiv m_A^2 = \mu_d^2 + \frac{1}{2}\lambda'' v_{SM}^2.$$

$$m_{h_1^+}^2 = 0, \quad m_{h_2^+}^2 = m_{h_3^+}^2 \equiv m_{h^+}^2 = \frac{1}{4}(2\mu_d^2 + \lambda_5 v_{SM}^2),$$

with $\lambda' = \lambda_5 + \lambda_6 + 2\lambda_7$ and $\lambda'' = \lambda_5 + \lambda_6 - 2\lambda_7$, where $\lambda_{5,6,7}$ are dimensionless coupling constants in the scalar potential. Note that μ_d^2 is not related to the spontaneous symmetry breaking and it is not protected by any symmetry, it may be larger than the electroweak scale. As we see in Eq.(3), h^+ and A^0 are the would-be Goldstone bosons that give masses to the W^\pm and Z gauge bosons and ϕ_k are the inert doublets. Due to the S_3 symmetry and the vacuum alignment, we have a residual symmetry and due to it, the mass eigenstates of the inert doublets are degenerate, as we can see in Eq. (3).

The residual symmetry, which implies in the masses degeneracy in Eq.(3), can be broken with soft terms in the scalar potential. So, adding the following quadratic terms $\nu_{nm}^2 H_n^\dagger H_m$, $n, m = 2, 3$ and imposing that $\nu_{22}^2 = \nu_{33}^2 = -\nu_{23}^2 \equiv \nu^2$, the mass matrix will remain diagonalized by the matrix, so the inert character is maintained. The eigenvalues are now:

$$\bar{m}_h^2 = m_h^2, \quad \bar{m}_{H_2}^2 = m_H^2, \quad \bar{m}_{H_3}^2 = m_H^2 + \nu^2,$$

$$\bar{m}_{A_1}^2 = 0, \quad \bar{m}_{A_2}^2 = m_A^2, \quad \bar{m}_{A_3}^2 = m_A^2 + \nu^2,$$

$$\bar{m}_{h_1^+}^2 = 0, \quad \bar{m}_{h_2^+}^2 = m_{h^+}^2, \quad \bar{m}_{h_3^+}^2 = m_{h^+}^2 + \nu^2, \quad (4)$$

where $m_h^2, m_A^2, m_{h^+}^2$ and m_H^2 are given in Eq. (3).

In the lepton and quark sectors all fields transform as singlet under S_3 , implying that they only interact with the singlet S as follows:

$$-\mathcal{L}_{Yukawa} = \bar{L}_{iL}(G_{ij}^l l_{jR} S + G_{ij}^\nu \nu_{jR} \tilde{S}) + \bar{Q}_{iL}(G_{ij}^u u_{jR} \tilde{S} + G_{ij}^d d_{jR} S) + H.c., \quad (5)$$

$\tilde{S} = i\tau_2 S^*$ and we have included right-handed neutrinos. For more details see [9].

The new inert scalar interactions with the gauge bosons, that arises from $(D_\mu \phi_i)^\dagger (D^\mu \phi_i)$ where $i = 1, 2$, used in our calculations are given by

$$\begin{aligned} \mathcal{L}_{Gauge} = & ig_{SW}(\partial_\mu h_i^- h_i^+ - \partial_\mu h_i^+ h_i^-)A^\mu + ig_{CW} \left(\frac{1-t_W^2}{2} \right) (\partial_\mu h_i^- h_i^+ - \partial_\mu h_i^+ h_i^-)Z^\mu \\ & + i \frac{g}{\sqrt{2}} (\partial_\mu h_i^- h_i^0 - \partial_\mu h_i^0 h_i^-)W^{+\mu} - i \frac{g}{\sqrt{2}} (\partial_\mu h_i^+ h_i^0 - \partial_\mu h_i^0 h_i^+)W^{-\mu} \\ & + g^2 s_W^2 h_i^- h_i^+ A_\mu A^\mu + g^2 c_W^2 \left(\frac{1-t_W^2}{2} \right)^2 h_i^- h_i^+ Z_\mu Z^\mu + 2g^2 s_W c_W \left(\frac{1-t_W^2}{2} \right) h_i^- h_i^+ A_\mu Z^\mu \\ & + \frac{g^2 s_W}{2} (h_i^- W_\mu^+ + h_i^+ W_\mu^-) h_i^0 A^\mu + \frac{g^2 c_W}{2} \left(\frac{1-t_W^2}{2} \right) (h_i^- W_\mu^+ + h_i^+ W_\mu^-) h_i^0 Z^\mu. \end{aligned} \quad (6)$$

The interactions between scalars are obtained from the following Lagrangian

$$\begin{aligned} \mathcal{L}_{Scalars} = & -\lambda_4 v_{SM} h^3 - \frac{\lambda_5 v_{SM}}{2} (h_2^- h_2^+ + h_3^- h_3^+) h + \lambda_8 v_{SM} (h_2^- h_2^+ - h_3^- h_3^+) h_3^0 - \frac{\lambda_8 v_{SM}}{2} (h_3^0)^3 \\ & - \frac{\lambda' v_{SM}}{2} h [(h_2^0)^2 + (h_3^0)^2] - \frac{\lambda_8 v_{SM}}{2} (h_2^0)^2 h_3^0 - \frac{\lambda_4}{4} h^4 - \lambda_8 v_{SM} h_2^0 (h_2^+ h_3^- + h_2^- h_3^+) - \frac{\lambda_8}{2} h (h_2^0)^2 h_3^0 \\ & - \frac{\lambda_8}{2} h (h_3^0)^3 + \lambda_8 h h_3^0 (h_2^- h_2^+ - h_3^- h_3^+) - \frac{\lambda'}{2} h^2 [(h_2^0)^2 + (h_3^0)^2] - 2\lambda_3 h_2^0 h_3^0 h_2^- h_3^+ - (\lambda_1 + \lambda_3) (h_3^0)^2 h_3^- h_3^+ \\ & - (\lambda_2 + \lambda_3) (h_2^- h_3^+)^2 - (\lambda_1 + \lambda_3) (h_2^- h_2^+)^2 - \frac{\lambda_1 + \lambda_3}{4} [(h_2^0)^4 + (h_3^0)^4] \\ & - (\lambda_1 + \lambda_3) (h_2^0)^2 (h_2^- h_2^+ + h_3^- h_3^+) - \lambda_8 h h_2^0 (h_2^- h_3^+ + h_2^+ h_3^-), \end{aligned} \quad (7)$$

where in particular the terms proportional to λ_5 are the couplings between the SM-Higgs with the charged scalars involved in the $h \rightarrow \gamma\gamma, \gamma Z$ decays. An special situation holds for some terms proportional to λ_8 as will be explained below.

III. PHENOMENOLOGY: RATIOS $R_{\gamma\gamma}$ AND $R_{\gamma Z}$

Recently, we have studied the IDMS₃ in the context where two, or one, of the new scalars were dark matter candidates, and we had shown two scenarios: 1) two of the scalars are mass degenerate and 2) there is no mass degeneracy. We are going to study the ratios $R_{\gamma\gamma}$ and $R_{\gamma Z}$ of the predictions of the IDMS₃ related to the SM.

To explore the sensitivity of the processes $h \rightarrow \gamma\gamma, \gamma Z$ due to new spin-0 content in the IDMS₃ we have used the experimental data reported by ATLAS and CMS collaborations. As can be seen in the Table I, $h \rightarrow \gamma\gamma$ is within 1σ related to the SM prediction, but for $h \rightarrow \gamma Z$ there is barely an upper limit of one order of magnitude above the SM prediction. For the Higgs decay in two photons see the experimental Ref. [5, 6], and for photon and Z Ref. [7, 8].

The S_3 symmetry and the vacuum alignment guarantee that the DM candidates do not decay into vector gauge bosons ($h_{2,3}^0 \rightarrow \gamma\gamma, \gamma Z$) through quantum fluctuations induced by new charged spin-0 content. It is important to note that this situation occurs in different ways for the candidates h_2^0 and h_3^0 . For h_2^0 , the S_3 symmetry directly forbids the existence of the couplings $h_2^0 h_2^+ h_2^-$ and $h_2^0 h_3^+ h_3^-$, see Eq. (7), and therefore there will not exist loop induced decay of h_2^0 into vector gauge bosons caused by the new charged scalars, as it occurs with the SM-Higgs h due to the presence of the couplings $h h_2^+ h_2^-$ and $h h_3^+ h_3^-$ proportional to λ_5 . For h_3^0 , the reason is quite different. Despite the existence of the vertices $h_3^0 h_2^+ h_2^-$ and $h_3^0 h_3^+ h_3^-$, the S_3 symmetry provides them with opposite signs, as can be seen explicitly from the third term in the scalar Lagrangian, $\lambda_8 v_{SM} (h_2^- h_2^+ - h_3^- h_3^+) h_3^0$, in consequence in the decays $h_3^0 \rightarrow \gamma\gamma, \gamma Z$ such spin-0 virtual contributions will cancel out each other in the degenerate scenario $m_{h_2^+} = m_{h_3^+}$. Or, it also can occur, in the non degenerate case, that those decays vanish if $\lambda_8 = 0$ in the scalar potential, as it was considered in Ref. [10]; and still if $\lambda_8 \ll 1$, then $h_3^0 \rightarrow \gamma\gamma, \gamma Z$ are highly suppressed.

As it is known, the Higgs's discovery channel is $pp \rightarrow gg \rightarrow h \rightarrow \gamma\gamma$, and because of the nature of the IDMS₃ the SM interactions between the Higgs and quarks remains intact, thus there are no novelties in the Higgs fabric side $pp \rightarrow gg \rightarrow h$. On the other hand, new physics effects could come from new spin-0 particles in the Higgs decay process. More specifically, because the cross section for the Higgs production $pp \rightarrow gg \rightarrow h$ is the same for the SM and the IDMS₃, the application of the narrow width approximation (NWA) at the resonant point (when the gluon

fusion energy is $\sqrt{\hat{s}} = m_h$), allow us to analyze the ratio signals with pure on-shell information

$$\begin{aligned}
R_{\gamma V} &\equiv \frac{\sigma(pp \rightarrow gg \rightarrow h \rightarrow \gamma V)^{\text{IDMS}_3}}{\sigma(pp \rightarrow gg \rightarrow h \rightarrow \gamma V)^{\text{SM}}} \\
&\stackrel{\text{NWA}}{\simeq} \frac{\sigma(gg \rightarrow h)^{\text{IDMS}_3} \text{Br}(h \rightarrow \gamma V)^{\text{IDMS}_3}}{\sigma(gg \rightarrow h)^{\text{SM}} \text{Br}(h \rightarrow \gamma V)^{\text{SM}}} \\
&= \frac{\Gamma(h \rightarrow \gamma V)^{\text{IDMS}_3}}{\Gamma(h \rightarrow \gamma V)^{\text{SM}}} \frac{\Gamma_h^{\text{SM}}}{\Gamma_h^{\text{IDMS}_3}}, \tag{8}
\end{aligned}$$

where $V \equiv \gamma, Z$. We would like to call attention that in our scenarios the new neutral scalar masses forbid invisible decays of the SM-Higgs, except in the scenario 1a of Table 1 of Ref. [10] in which at the Born level yields $\Gamma(h \rightarrow h_3^0 h_3^0) \sim 10^{-6}$ GeV, which is highly suppressed and does not disturb the total Higgs width, hence $\Gamma_h^{\text{IDMS}_3} \simeq \Gamma_h^{\text{SM}}$, leading to

$$R_{\gamma V} = \frac{\Gamma(h \rightarrow \gamma V)^{\text{IDMS}_3}}{\Gamma(h \rightarrow \gamma V)^{\text{SM}}}. \tag{9}$$

As we have seen, the IDMS₃ gives rise to couplings between the new charged scalars and the SM-Higgs boson, and also with vector gauge bosons, but there are no modifications to the existing SM couplings, therefore for the decays $h \rightarrow \gamma\gamma, \gamma Z$ only a new scalar contribution is added to the existing ones.

The participating diagrams in the processes $h \rightarrow \gamma\gamma, \gamma Z$ are illustrated in the Fig. 1 in the unitary gauge, where (a) corresponds to fermions, (b) and (c) to W gauge boson, and (d) and (e) to new charged scalars. We have constructed each diagram and performed the loop integrals with the Passarino-Veltman reduction method [26] using **FeynCalc** [27] obtaining the results in terms of the scalar functions B_0 and C_0 [28]. We have also calculated their corresponding general analytical solutions, which lead to the known standard notations of Refs. [29–31]. Particularly here we work with the Djouadi notation [30, 31] for the width decays. In the Appendix we report the amplitudes of the processes and give details of the correspondence between our direct results in terms of the B_0 and C_0 functions and the Djouadi notation.

In the following we present the width decays showing explicitly only the new spin-0 contribution of the model. The other known spin-1/2 and spin-1 contributions are given in the Appendix.

The Higgs decay into two photons has new spin-0 contribution given by

$$\Gamma(h \rightarrow \gamma\gamma) = \frac{G_F \alpha^2 m_h^3}{128 \sqrt{2} \pi^3} \left| \sum_{i=1}^9 N_C^{f_i} Q_{f_i}^2 A_{1/2}^{\gamma\gamma}(\tau_{f_i}) + A_1^{\gamma\gamma}(\tau_W) + \frac{\lambda_5 v_{SM}^2}{2} \sum_{i=2}^3 \frac{1}{m_{h_i^\pm}^2} A_0^{\gamma\gamma}(\tau_{h_i^\pm}) \right|^2, \tag{10}$$

with the form factors $A_{\text{Spin}}^{\gamma\gamma}$, where the charged scalar form factor is

$$A_0^{\gamma\gamma} \equiv -[\tau_{h^\pm} - f(\tau_{h^\pm})] \tau_{h^\pm}^{-2}, \tag{11}$$

the $f(\tau)$ function is presented in the Appendix.

The Higgs decay into photon and Z has also new spin-0 contribution

$$\Gamma(h \rightarrow \gamma Z) = \frac{G_F^2 m_W^2 \alpha m_h^3}{64 \pi^4} \left(1 - \frac{m_Z^2}{m_h^2} \right)^3 \left| \frac{2}{c_W} \sum_{i=1}^9 N_C^{f_i} Q_{f_i} g_V^{f_i} A_{1/2}^{\gamma Z}(\tau_{f_i}) + A_1^{\gamma Z}(\tau_W) + \frac{\lambda_5 v_{SM}^2 v_{h^\pm}}{2} \sum_{i=2}^3 \frac{1}{m_{h_i^\pm}^2} A_0^{\gamma Z}(\tau_{h_i^\pm}) \right|^2, \tag{12}$$

where $v_{h^\pm} \equiv c_W(1 - t_W^2)$, $A_{\text{Spin}}^{\gamma Z}$ are the form factors, with the new charged scalar contribution

$$A_0^{\gamma Z} \equiv -I_1, \tag{13}$$

see the Appendix for detailed information about all the form factors and the $I_{1,2}$ auxiliary definitions, and also about the $f(\tau)$ and $g(\tau)$ functions and their relations with the Passarino-Veltman scalar functions.

In the next section we report our phenomenological analysis for $h \rightarrow \gamma\gamma, \gamma Z$. We use the values $m_h = 125.7$ GeV with the more recent data from PDG Live (september 2014): $m_W = 80.385$, $m_Z = 91.1876$, $m_u = 0.0023$, $m_d = 0.0048$, $m_s = 0.095$, $m_c = 1.275$, $m_b = 4.18$, $m_t = 173.07$, $m_e = 0.000511$, $m_\mu = 0.105658$, $m_\tau = 1.77682$, all values in GeV, $G_F = 1.1663787 \times 10^{-5}$ GeV⁻².

IV. RESULTS

The four collaborations of LEP [33] and ATLAS [34] have searched for charged scalars. Notwithstanding, their lower limits depend on the model which is always the two Higgs doublet model (2HDM). In LEP experiments, the searches include 2HDM of type I and II. Type I is searched in the ATLAS experiment. Both searches depend on the assumed branching ratio of the charged Higgs boson decays. ATLAS, for instance, assume $H^+ \rightarrow c\bar{s} = 100\%$. Summarizing, ATLAS has observed no signal for H^+ masses between 90 GeV and 150 GeV and LEP has excluded this sort of scalars with mass below 72.5 GeV for type I scenario and 80 GeV for the type II scenario. However, none of these results applies to our model since the charged scalar are inert and do not couple to fermions. Anyway, we will use 80 GeV for the mass of h_2^+ which is in the range of LEP and ATLAS results. For the other charged scalar, h_3^+ we will obtain a lower limit for its mass using its contribution to the Z boson invisible decay width, where we have found $m_{h_3^+} > 25$ GeV, if we consider a 3σ deviation for the invisible decay width in our calculations. These result can be appreciated in Fig. 2.

We first report the $h \rightarrow \gamma\gamma$ channel, and for the experimental comparison we use the data provided by ATLAS [5] and CMS [6] collaborations, given in Table I. We had chosen the wider interval available for the $h \rightarrow \gamma\gamma$ process, this is, the $R_{\gamma\gamma}^{\text{ATLAS,CMS}} \pm 1\sigma$, the namely Maximum $R_{\gamma\gamma}^{\text{ATLAS,CMS}} + 1\sigma = 1.4$ and the Minimum $R_{\gamma\gamma}^{\text{ATLAS,CMS}} - 1\sigma = 0.9$.

In the Fig. 3 we present $R_{\gamma\gamma}$ with $m_{h_2^+} = 80$ GeV. First, we show $R_{\gamma\gamma}$ as function of $m_{h_3^+}$, in Fig. 3(a) we consider λ_5 negative and in Fig. 3(b) positive, where the vertical line indicates the mass limit $m_{h_3^+} > 25$ GeV imposed by the Z invisible decay width; in Fig. 3(c) $R_{\gamma\gamma}$ is presented as function of $-0.5 \leq \lambda_5 \leq 0.5$ and different values of $m_{h_3^+}$ are chosen. From the three plots it can be appreciated that negative values of λ_5 and $m_{h_3^+} > m_h/2$ favours a positive deviation signal, being more compatible with the experimental allowed region if $m_{h_3^+} > 80$ GeV. For positive values of λ_5 and $m_{h_3^+} < m_h/2$ there is also a compatible positive deviation, but this mass scenario for the charged scalars could not be valid if the experimental values for one charged scalar mass limit from LEP [33] and ATLAS [34] are also valid for an extra charged scalar h_3^+ . If future experimental data confirms a small negative deviation for $R_{\gamma\gamma}$, the S_3 model still has room for consistency with a scenario of positive $\lambda_5 \simeq 0.1$ and $m_{h_{2,3}^+} > 80$ GeV.

Considering $R_{\gamma Z}$, we have also made an analysis entirely analogous to the two photons case. For the $h \rightarrow \gamma Z$ process, the available experimental data is still very rough, ATLAS [7] and CMS [8] collaborations provide so far upper limits of one order of magnitude larger than the SM prediction, see Table I. In Fig. 4 we illustrate the $R_{\gamma Z}$ results, where essentially this ratio has the same shape and behaviour considering the parameters λ_5 and $m_{h_{2,3}^+}$ related to the the two photons case, except that now the signal is more suppressed. This result is congruent because the $h \rightarrow \gamma\gamma$ decay has massless particles in the final state while the process $h \rightarrow \gamma Z$ produces one heavy particle. So, it is expected that the latter process is a little bit less sensitive to the common parameters λ_5 and $m_{h_{2,3}^+}$ if compared to the two photons channel. Then, the signal for the $R_{\gamma\gamma}$ compatible with the experimental data, should be larger than the corresponding $R_{\gamma Z}$. Therefore, in our results, all analysis derived from the $h \rightarrow \gamma\gamma$ decay also apply to the process $h \rightarrow \gamma Z$, where the scenario of negative λ_5 and $m_{h_{2,3}^+} > 80$ GeV agrees mostly within the more accurate experimental data.

Since both processes depend on the same parameters λ_5 and $m_{h_{2,3}^+}$, it is necessary to explore the correlation between them. Fig. 5 presents the correlation between the ratios $R_{\gamma\gamma}$ and $R_{\gamma Z}$ as function of $-0.5 \leq \lambda_5 \leq 0.5$, with $m_{h_2^+} = 80$ GeV and different values of $m_{h_3^+}$. Notice that we explicitly trace the most accurate available experimental data for the two photon process, and we discard to trace the currently rough upper limits reported for the photon and Z process. In Fig. 5(a) we set $m_{h_3^+} = 25$ GeV and it can be seen that mainly negative values of λ_5 satisfy the experimental data for $R_{\gamma\gamma}$ but, as commented before, ATLAS [34] has excluded a mass below 80 GeV for at least one charged scalar. In the Figs. 5 (b), (c) and (d) the values $m_{h_3^+} = 80, 160$ and 320 GeV were respectively considered, and the best fit within the allowed experimental region are for the negative values of λ_5 , even more if $m_{h_2^+} < m_{h_3^+}$.

The Fig. 6 shows the correlation as function of the $80 \leq m_{h_2^+} \leq 500$ GeV, considering $\lambda_5 = \pm 0.4$ and different values of $m_{h_3^+}$. In Fig. 6(a) the scenario $m_{h_3^+} = 25$ GeV is incompatible with the allowed region. In Fig. 6(b), (c) and (d) we work with the respective scenarios $m_{h_3^+} = 80, 160$ and 320 GeV, the curves for $R_{\gamma\gamma}$ fits manly with the data when $\lambda_5 = -0.4$ is considered.

The Fig. 7 shows the correlation as function of $80 \leq m_{h_2^+} \leq 500$ GeV, with $\lambda_5 = \pm 0.4$, but here $m_{h_3^+}$ maintains a proportionality with $m_{h_2^+}$. Notice that in all this plots the two line segments converge to $R_{\gamma\gamma} = 1$, in 7(a) the degenerate case $m_{h_3^+} = m_{h_2^+}$ is considered, in 7(b) $m_{h_3^+} = 2m_{h_2^+}$, and in 7(c) $m_{h_3^+} = 4m_{h_2^+}$. Once more, it can be appreciated that a negative value $\lambda_5 = -0.4$ is more compatible with the experimental allowed region, and the heavier $m_{h_2^+}$ is the closer to the SM prediction, or, in other words, the charged scalars decouple.

The Fig. 8 presents contour plots of $R_{\gamma\gamma}$ and $R_{\gamma Z}$ as function of $m_{h_{2,3}^+} \geq 80$ GeV and λ_5 . In Fig. 8(a) with $\lambda_5 = -0.4$ is favored a positive deviation and in Fig. 8(b) with $\lambda_5 = 0.4$ a negative deviation occurs. More specifically, here we have the opportunity to appreciate in a same plot the behavior of both processes, and is clear that $R_{\gamma\gamma}$ is more sensitive to the same parameters than $R_{\gamma Z}$, whether λ_5 has positive or negative value. Or, in other words, the impact of the parameters λ_5 and $m_{h_{2,3}^+}$ on $R_{\gamma Z}$ is always less significant than in $R_{\gamma\gamma}$.

V. CONCLUSIONS

In this work we have considered the SM-like Higgs scalar decaying in $\gamma\gamma$ and γZ in the context of the IDMS₃ model. Both decays may have ratios $R_{\gamma\gamma}$ and $R_{\gamma Z}$ that can be enhanced or suppressed compared to the values predicted by the SM. It can be noted that the signal of the λ_5 parameter is the most responsible for this positive or negative deviation. The shape and behaviour of both curves are very similar, and the difference of them is due to the massive particle in the final state of the $h \rightarrow \gamma Z$ channel, therefore it is expected that the latter process be less sensitive than the two photons channel related to the common parameters λ_5 and $m_{h_{2,3}^+}$. The lower value for $m_{h_3^+}$ was obtained from the limit established for the $Z \rightarrow h_3^+ h_3^-$ invisible decay. Thus, our parameters are safe by considering this limit. We would like to stress that in the present model both charged scalars $h_{2,3}^+$ do not couple to fermions. The lower limit obtained by LEP and LHC does not apply in this case. However, we use $m_{h_2^+} > 80$ GeV from ATLAS [34].

Working with a fixed $m_{h_3^+}$ and varying λ_5 , both ratios behave very similar, but notice that the reported upper limit for $R_{\gamma Z}$ is too high to be reached with the chosen parameters. On the other hand, the predicted value for $R_{\gamma\gamma}$ is reached with our parameter choice. We have concentrated in $\lambda_5 \in [-0.4, +0.4]$ due to consistence with the results of Ref. [10] where we had shown reasonable values of this model that can accommodate dark matter candidates.

Regarding the signal of the λ_5 parameter, we would like to call the attention to a similar analysis that had been done in the context of a general three Higgs doublets with S_3 symmetry, but without inert doublets, in Ref. [25]. In this case, both decays only have a suppression compared to the SM value: $R_{\gamma\gamma} \in [0.42, 0.80]$ and $R_{\gamma Z} \in [0.73, 0.93]$. The difference between our analysis and the one of Ref. [25] is that in our case the μ_d^2 parameter does not contribute to the spontaneous symmetry breaking. In our case, the masses of the scalars are not limited by v_{SM}^2 and by λ 's of the scalar potentials, this allow positive and negative values for λ_5 , whereas in [25] the respective parameter is always negative. See the Eq. (46) in the latter reference. Our analysis is congruent with theirs when λ_5 is positive. An earlier analysis, also about the parameter space of both ratios in the IDM model, can be found in [24].

It is interesting to note that in the IDMS₃ when our $R_{\gamma\gamma}$ reaches the maximum allowed value $R_{\gamma\gamma}^{\text{ATLAS,CMS}} + 1\sigma = 1.4$, then from the correlation plots can be appreciated that our higher prediction for the positive deviation of the $h \rightarrow \gamma Z$ channel is $R_{\gamma Z} \approx 1.2$. This behaviour has been observed in other multi-Higgs models which include a real [35] or complex [36] triplets. Otherwise, in case that future experimental reports show a deviation up to one order of magnitude for the photon and Z channel compared to the SM prediction, it could be due to new physics effects that maybe requires a different coupling of the new particle with the Z boson. For sure it will be an invitation to revisit the status of the SM.

Appendix: Form factors in terms of the Passarino–Veltman scalar functions

Here we present explicitly the form factors A_{Spin} [30, 31], given in Eqs. (10) and (12), in terms of the B_0 and C_0 Passarino-Veltman scalar functions [28]. We have constructed and solved each loop diagram with the Passarino-Veltman reduction method [26] using `FeynCalc` [27], and also obtained the corresponding analytical solutions for the B_0 and C_0 scalar integrals via the Feynman parametrization method [26, 37–39], the solutions have been verified numerically using `LoopTools` [40].

For the $h \rightarrow \gamma\gamma$ decay, with configuration $h(p_3) \rightarrow \gamma_{\mu_1}(p_1)\gamma_{\mu_2}(p_2)$, the amplitude is

$$\mathcal{M}_{h \rightarrow \gamma\gamma} = \mathcal{M}_{\gamma\gamma}^{\mu_1\mu_2} \epsilon_{\mu_1}^*(p_1, \lambda_1) \epsilon_{\mu_2}^*(p_2, \lambda_2), \quad (\text{A.1})$$

with kinematics $p_3 = p_1 + p_2$, $p_3^2 = m_h^2$, $p_1^2 = p_2^2 = 0$, $p_1 \cdot p_2 = m_h^2/2$, and transversality conditions $p_1^{\mu_1} = p_2^{\mu_2} = 0$. The tensorial amplitude is

$$\begin{aligned} \mathcal{M}_{\gamma\gamma}^{\mu_1\mu_2} = & -i \frac{\sqrt{2}G_F}{2\pi} \alpha \left[\sum_{i=1}^9 N_C^{f_i} Q_{f_i}^2 A_{1/2}^{\gamma\gamma}(\tau_{f_i}) + A_1^{\gamma\gamma}(\tau_W) + \frac{\lambda_5 v_{SM}^2}{2} \sum_{i=2}^3 \frac{1}{m_{h_i^+}^2} A_0^{\gamma\gamma}(\tau_{h_i^+}) \right] \\ & \times \left(\frac{m_h^2}{2} g^{\mu_1\mu_2} - p_2^{\mu_1} p_1^{\mu_2} \right), \end{aligned} \quad (\text{A.2})$$

where $\tau_X \equiv m_h^2/4m_X^2$ and $X = f, W, h^\pm$, with the form factors are

$$\begin{aligned} A_{1/2}^{\gamma\gamma} &\equiv \frac{4m_f^2}{m_h^2} \left[2 + (4m_f^2 - m_h^2) C_0^{h,f} \right] \\ &= 2[\tau_f + (\tau_f - 1)f(\tau_f)]\tau_f^{-2}, \end{aligned} \quad (\text{A.3})$$

$$\begin{aligned} A_1^{\gamma\gamma} &\equiv -2 \left\{ 1 + 6 \frac{m_W^2}{m_h^2} \left[1 + (2m_W^2 - m_h^2) C_0^{h,W} \right] \right\} \\ &= -[2\tau_W^2 + 3\tau_W + 3(2\tau_W - 1)f(\tau_W)]\tau_W^{-2}, \end{aligned} \quad (\text{A.4})$$

$$\begin{aligned} A_0^{\gamma\gamma} &\equiv -\frac{4m_{h^+}^2}{m_h^2} \left(1 + 2m_{h^+}^2 C_0^{h,h^+} \right) \\ &= -[\tau_{h^+} - f(\tau_{h^+})]\tau_{h^+}^{-2}, \end{aligned} \quad (\text{A.5})$$

$$f(\tau) \equiv \begin{cases} \arcsin^2 \sqrt{\tau} & , \tau \leq 1 \\ -\frac{1}{4} \left(\log \frac{1+\sqrt{1-\tau^{-1}}}{1-\sqrt{1-\tau^{-1}}} - i\pi \right)^2 & , \tau > 1 \end{cases}, \quad \tau \equiv \frac{m_h^2}{4m_X^2}. \quad (\text{A.6})$$

The three-point Passarino-Veltman scalar function is

$$\begin{aligned} C_0^{h,X} &\equiv C_0(0, 0, m_h^2, m_X^2, m_X^2, m_X^2) \\ &= -\frac{2}{m_h^2} \arctan^2 \frac{-i}{\sqrt{1 - \frac{4m_X^2}{m_h^2}}} \\ &= -\frac{2}{m_h^2} f(\tau). \end{aligned} \quad (\text{A.7})$$

For the $h \rightarrow \gamma Z$ decay, with configuration $h(p_3) \rightarrow \gamma_{\mu_1}(p_1)Z_{\mu_2}(p_2)$, the amplitude is

$$\mathcal{M}_{\gamma Z} = \mathcal{M}_{\gamma Z}^{\mu_1 \mu_2} \epsilon_{\mu_1}^*(p_1, \lambda_1) \epsilon_{\mu_2}^*(p_2, \lambda_2), \quad (\text{A.8})$$

with kinematics $p_3 = p_1 + p_2$, $p_3^2 = m_h^2$, $p_1^2 = 0$, $p_2^2 = m_Z^2$, $p_1 \cdot p_2 = (m_h^2 - m_Z^2)/2$, and transversality conditions $p_1^{\mu_1} = p_2^{\mu_2} = 0$. The tensorial amplitude is

$$\begin{aligned} \mathcal{M}_{h \rightarrow \gamma Z}^{\mu_1 \mu_2} &= i \frac{\sqrt{\alpha} G_F m_W}{\sqrt{2} \pi^{3/2}} \left[\frac{2}{c_W} \sum_{i=1}^9 N_C^{f_i} Q_{f_i} g_V^{f_i} A_{1/2}^{\gamma Z}(\tau_{f_i}) + A_1^{\gamma Z}(\tau_W) + \frac{\lambda_5 v_{SM}^2 v_{h^\pm}}{2} \sum_{i=2}^3 \frac{1}{m_{h_i^+}^2} A_0^{\gamma Z}(\tau_{h_i^+}) \right] \\ &\quad \times \left(\frac{m_h^2 - m_Z^2}{2} g^{\mu_1 \mu_2} - p_2^{\mu_1} p_1^{\mu_2} \right), \end{aligned} \quad (\text{A.9})$$

where $\tau_X \equiv 4m_X^2/m_h^2$, $\lambda_X \equiv 4m_X^2/m_Z^2$ and $X = f, W, h^\pm$, with the form factors

$$\begin{aligned} A_{1/2}^{\gamma Z} &= -\frac{2m_f^2}{m_h^2 - m_Z^2} - \frac{2m_Z^2 m_f^2}{(m_h^2 - m_Z^2)^2} (B_0^{h,f} - B_0^{Z,f}) + m_f^2 \left(1 - \frac{4m_f^2}{m_h^2 - m_Z^2} \right) C_0^{h,Z,f} \\ &= I_1(\tau_f, \lambda_f) - I_2(\tau_f, \lambda_f), \end{aligned} \quad (\text{A.10})$$

$$\begin{aligned} A_1^{\gamma Z} &= \frac{1}{m_W m_Z (m_h^2 - m_Z^2)^2} \left\{ [2m_W^2(m_h^2 + 6m_W^2) - m_Z^2(m_h^2 + 2m_W^2)] [m_h^2 - m_Z^2 + m_Z^2 (B_0^{h,W} - B_0^{Z,W})] \right. \\ &\quad \left. + 2(m_h^2 - m_Z^2) m_W^2 [6m_W^2(2m_W^2 + m_Z^2) - 2m_h^4 + m_h^2(m_Z^2 - 6m_W^2)] C_0^{h,Z,W} \right\} \\ &= c_W \{ 4(3 - t_W^2) I_2(\tau_W, \lambda_W) + [(1 + 2\tau_W^{-1}) t_W^2 - (5 + 2\tau_W^{-1})] I_1(\tau_W, \lambda_W) \}, \end{aligned} \quad (\text{A.11})$$

$$\begin{aligned}
A_0^{\gamma Z} &= \frac{2m_{h^+}^2}{(m_h^2 - m_Z^2)^2} \left[m_Z^2 \left(B_0^{h,h^+} - B_0^{Z,h^+} \right) + (m_h^2 - m_Z^2) \left(1 + 2m_{h^+}^2 C_0^{h,Z,h^+} \right) \right] \\
&= -I_1(\tau_{h^+}, \lambda_{h^+}) ,
\end{aligned} \tag{A.12}$$

and the auxiliary functions

$$\begin{aligned}
I_1(\tau, \lambda) &\equiv \frac{\tau\lambda}{2(\tau - \lambda)} + \frac{\tau^2\lambda^2}{2(\tau - \lambda)^2} [f(\tau^{-1}) - f(\lambda^{-1})] + \frac{\tau^2\lambda}{(\tau - \lambda)^2} [g(\tau^{-1}) - g(\lambda^{-1})] , \\
I_2(\tau, \lambda) &\equiv -\frac{\tau\lambda}{2(\tau - \lambda)} [f(\tau^{-1}) - f(\lambda^{-1})] ,
\end{aligned} \tag{A.13}$$

we emphasize that here $\tau \equiv 4m_X^2/m_h^2$, opposite to the two photons case, therefore here $f(\tau^{-1})$ evaluates $\tau^{-1} = m_h^2/4m_X^2$ for consistency because originally $f(\tau)$ is defined in Eq. (A.6) with $\tau \equiv m_h^2/4m_X^2$, and exactly the same situation holds for

$$g(\tau) \equiv \begin{cases} \sqrt{\tau^{-1} - 1} \arcsin \sqrt{\tau} & , \tau \leq 1 \\ \frac{\sqrt{1 - \tau^{-1}}}{2} \left(\log \frac{1 + \sqrt{1 - \tau^{-1}}}{1 - \sqrt{1 - \tau^{-1}}} - i\pi \right) & , \tau > 1 \end{cases} , \quad \tau \equiv \frac{m_h^2}{4m_X^2} , \tag{A.14}$$

where we disagree with the inequalities orientations given in Refs. [30, 31], but the correct definition can be found in the same author's Ref. [32], as also used in Ref. [17].

The two-point scalar function, of divergent nature, is

$$\begin{aligned}
B_0^{h,X} &= B_0(m_h^2, m_X^2, m_X^2) \\
&= \Delta - \log \frac{m_X^2}{\mu^2} + 2 - 2i \sqrt{1 - \frac{4m_X^2}{m_h^2}} \arctan \frac{-i}{\sqrt{1 - \frac{4m_X^2}{m_h^2}}} \\
&= \Delta - \log \frac{m_X^2}{\mu^2} + 2 - 2g(\tau) ,
\end{aligned} \tag{A.15}$$

$$\Delta \equiv \frac{2}{4 - D} - \gamma_E + \log 4\pi , \tag{A.16}$$

where $g(\tau)$ is accordingly with Eq. (A.14), and the difference of two B_0 with same virtual masses yields the finite result

$$B_0^{h,X} - B_0^{Z,X} = -2[g(\tau) - g(\lambda)] . \tag{A.17}$$

The **LoopTools** program evaluates all B_0 without the $\Delta + \log \mu^2$ term by default because in all finite result such terms must vanish, as in Eq. (A.17).

Finally, the last three-point scalar function is

$$\begin{aligned}
C_0^{h,Z,X} &\equiv C_0(0, m_h^2, m_Z^2, m_X^2, m_X^2, m_X^2) \\
&= \frac{m_h^2 C_0^{h,X} - m_Z^2 C_0^{Z,X}}{m_h^2 - m_Z^2} \\
&= \frac{-2}{m_h^2 - m_Z^2} [f(\tau) - f(\lambda)] ,
\end{aligned} \tag{A.18}$$

where $C_0^{h,X}$ and $C_0^{Z,X}$ are given in Eq. (A.7).

Acknowledgments

ACBM thanks CAPES for financial support. ECFSF and JM thanks to FAPESP for financial support under the respective processes number 2011/21945-8 and 2013/09173-5. VP thanks to CNPq for partial support.

JM would like to thank to Bogumiła Świeżewska for the valuable discussion.

-
- [1] G. Aad *et al.* [ATLAS Collaboration], arXiv:1307.1432 [hep-ex]; G. Aad *et al.* [ATLAS Collaboration]: ATLAS-CONF-2013-040.
 - [2] S. Chatrchyan *et al.* [CMS Collaboration], Phys. Rev. Lett. **110**, 081803 (2013) [arXiv:1212.6639 [hep-ex]]. CMS-PAS-HIG-13-002.
 - [3] G. Aad *et al.* [ATLAS Collaboration], Phys. Lett. B **716**, 1 (2012) [arXiv:1207.7214 [hep-ex]].
 - [4] S. Chatrchyan *et al.* [CMS Collaboration], Phys. Lett. B **716**, 30 (2012) [arXiv:1207.7235 [hep-ex]].
 - [5] G. Aad *et al.* [ATLAS Collaboration], arXiv:1408.7084 [hep-ex].
 - [6] V. Khachatryan *et al.* [CMS Collaboration], arXiv:1407.0558 [hep-ex].
 - [7] G. Aad *et al.* [ATLAS Collaboration], Phys. Lett. B **732**, 8 (2014) [arXiv:1402.3051 [hep-ex]].
 - [8] S. Chatrchyan *et al.* [CMS Collaboration], Phys. Lett. B **726**, 587 (2013) [arXiv:1307.5515 [hep-ex]].
 - [9] A. C. B. Machado and V. Pleitez, arXiv:1205.0995 [hep-ph].
 - [10] E. C. F. S. Fortes, A. C. B. Machado, J. Montaña and V. Pleitez, arXiv:1407.4749 [hep-ph].
 - [11] M. Gustafsson, S. Rydbeck, L. Lopez-Honorez and E. Lundstrom, Phys. Rev. D **86**, 075019 (2012) [arXiv:1206.6316 [hep-ph]].
 - [12] A. Goudelis, B. Herrmann and O. Stål, JHEP **1309**, 106 (2013) [arXiv:1303.3010 [hep-ph]].
 - [13] L. Lopez Honorez and C. E. Yaguna, JCAP **1101** (2011) 002 [arXiv:1011.1411 [hep-ph]].
 - [14] L. Lopez Honorez, E. Nezri, J. F. Oliver and M. H. G. Tytgat, JCAP **0702**, 028 (2007) [hep-ph/0612275].
 - [15] T. Hambye and M. H. G. Tytgat, Phys. Lett. B **659**, 651 (2008) [arXiv:0707.0633 [hep-ph]].
 - [16] A. Arhrib, R. Benbrik and N. Gaur, Phys. Rev. D **85**, 095021 (2012) [arXiv:1201.2644 [hep-ph]].
 - [17] B. Świeżewska and M. Krawczyk, Phys. Rev. D **88**, 035019 (2013) [arXiv:1212.4100 [hep-ph]].
 - [18] E. Lundstrom, M. Gustafsson and J. Edsjo, Phys. Rev. D **79**, 035013 (2009) [arXiv:0810.3924 [hep-ph]].
 - [19] Q. -H. Cao, E. Ma and G. Rajasekaran, Phys. Rev. D **76**, 095011 (2007) [arXiv:0708.2939 [hep-ph]].
 - [20] E. Dolle, X. Miao, S. Su and B. Thomas, Phys. Rev. D **81**, 035003 (2010) [arXiv:0909.3094 [hep-ph]].
 - [21] R. Barbieri, L. J. Hall and V. S. Rychkov, Phys. Rev. D **74**, 015007 (2006) [hep-ph/0603188].
 - [22] H. Davoudiasl and I. M. Lewis, Phys. Rev. D **90**, 033003 (2014) [arXiv:1404.6260 [hep-ph]].
 - [23] C. -S. Chen, C. -Q. Geng, D. Huang and L. -H. Tsai, Phys. Rev. D **87**, 075019 (2013) [arXiv:1301.4694 [hep-ph]].
 - [24] M. Krawczyk, D. Sokołowska, P. Swaczyna and B. Świeżewska, Acta Phys. Polon. B **44**, no. 11, 2163 (2013) [arXiv:1309.7880 [hep-ph]].
 - [25] D. Das and U. K. Dey, Phys. Rev. D **89**, 095025 (2014) [arXiv:1404.2491 [hep-ph]].
 - [26] G. Passarino and M. J. G. Veltman, Nucl. Phys. B **160**, 151 (1979).
 - [27] R. Mertig, M. Bohm and A. Denner, Comput. Phys. Commun. **64**, 345 (1991).
 - [28] G. 't Hooft and M. J. G. Veltman, Nucl. Phys. B **153**, 365 (1979).
 - [29] J. F. Gunion, H. E. Haber, G. L. Kane and S. Dawson, Front. Phys. **80**, 1 (2000).
 - [30] A. Djouadi, Phys. Rept. **457**, 1 (2008) [hep-ph/0503172].
 - [31] A. Djouadi, Phys. Rept. **459**, 1 (2008) [hep-ph/0503173].
 - [32] M. Spira, A. Djouadi, D. Graudenz and P. M. Zerwas, Nucl. Phys. B **453**, 17 (1995) [hep-ph/9504378].
 - [33] G. Abbiendi *et al.* [ALEPH and DELPHI and L3 and OPAL and LEP Collaborations], Eur. Phys. J. C **73**, 2463 (2013) [arXiv:1301.6065 [hep-ex]].
 - [34] G. Aad *et al.* [ATLAS Collaboration], Eur. Phys. J. C **73**, 2465 (2013) [arXiv:1302.3694 [hep-ex]].
 - [35] C. Arina, V. Martin-Lozano and G. Nardini, JHEP **1408**, 015 (2014) [arXiv:1403.6434 [hep-ph]].
 - [36] C. H. Chen and T. Nomura, JHEP **1409**, 120 (2014) [arXiv:1404.2996 [hep-ph]].
 - [37] M. E. Peskin and D. V. Schroeder, “An Introduction to quantum field theory,” Reading, USA: Addison-Wesley (1995) 842 p
 - [38] D. Y. Bardin and G. Passarino, “The standard model in the making: Precision study of the electroweak interactions,” (International series of monographs on physics. 104)
 - [39] M. Bohm, A. Denner and H. Joos, “Gauge theories of the strong and electroweak interaction,” Stuttgart, Germany: Teubner (2001) 784 p
 - [40] T. Hahn and M. Perez-Victoria, Comput. Phys. Commun. **118**, 153 (1999) [hep-ph/9807565].

Ratio	ATLAS	CMS
$R_{\gamma\gamma}$	$1.17^{+0.27}_{-0.27}$ [5]	$1.14^{+0.26}_{-0.23}$ [6]
$R_{\gamma Z}$	< 11 [7]	< 9.5 [8]

TABLE I: Ratios of the experimental measured values compared to the SM predictions reported by ATLAS and CMS.

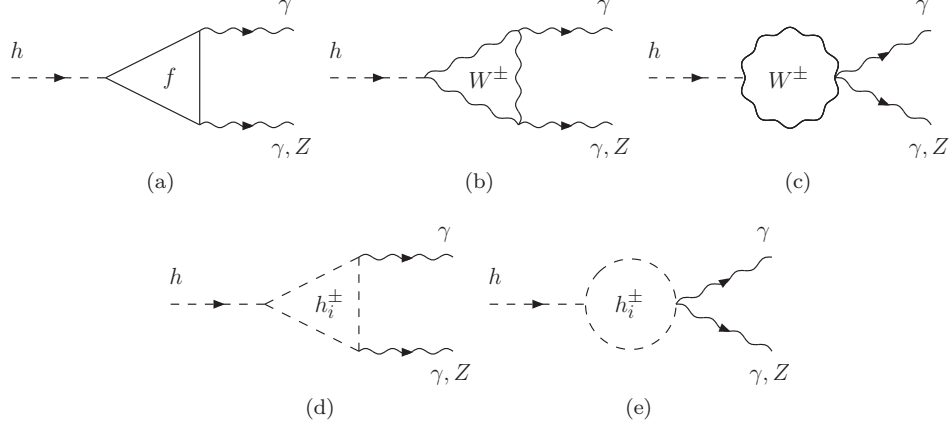


FIG. 1: Decays $h \rightarrow \gamma\gamma, \gamma Z$.

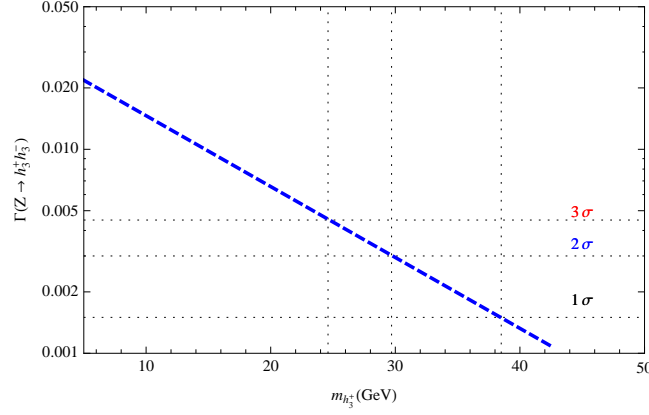


FIG. 2: Z invisible decay width, as a function of the charged scalar h_3^\pm mass. Imposing the error of the current value for the invisible decay as the allowed limit for the decay width we obtain a lower limit for the charged mass of 25 GeV.

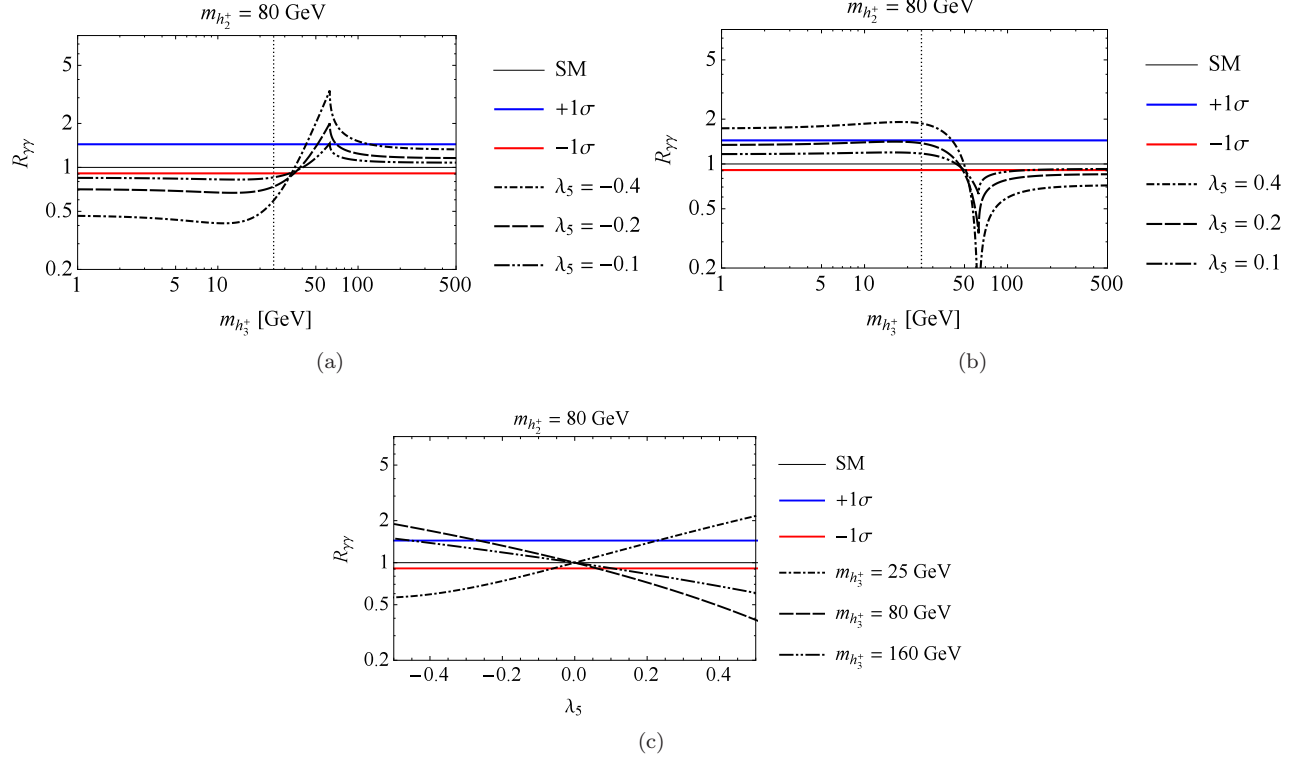


FIG. 3: $R_{\gamma\gamma}$ for $m_{h_2^+} = 80$ GeV fixed. In (a) and (b) consider $R_{\gamma\gamma}$ as function of $m_{h_3^+}$, but in (a) λ_5 is negative and in (b) is positive. In (c) $R_{\gamma\gamma}$ is presented as function of $-0.5 \leq \lambda_5 \leq 0.5$ with different values of $m_{h_3^+}$.

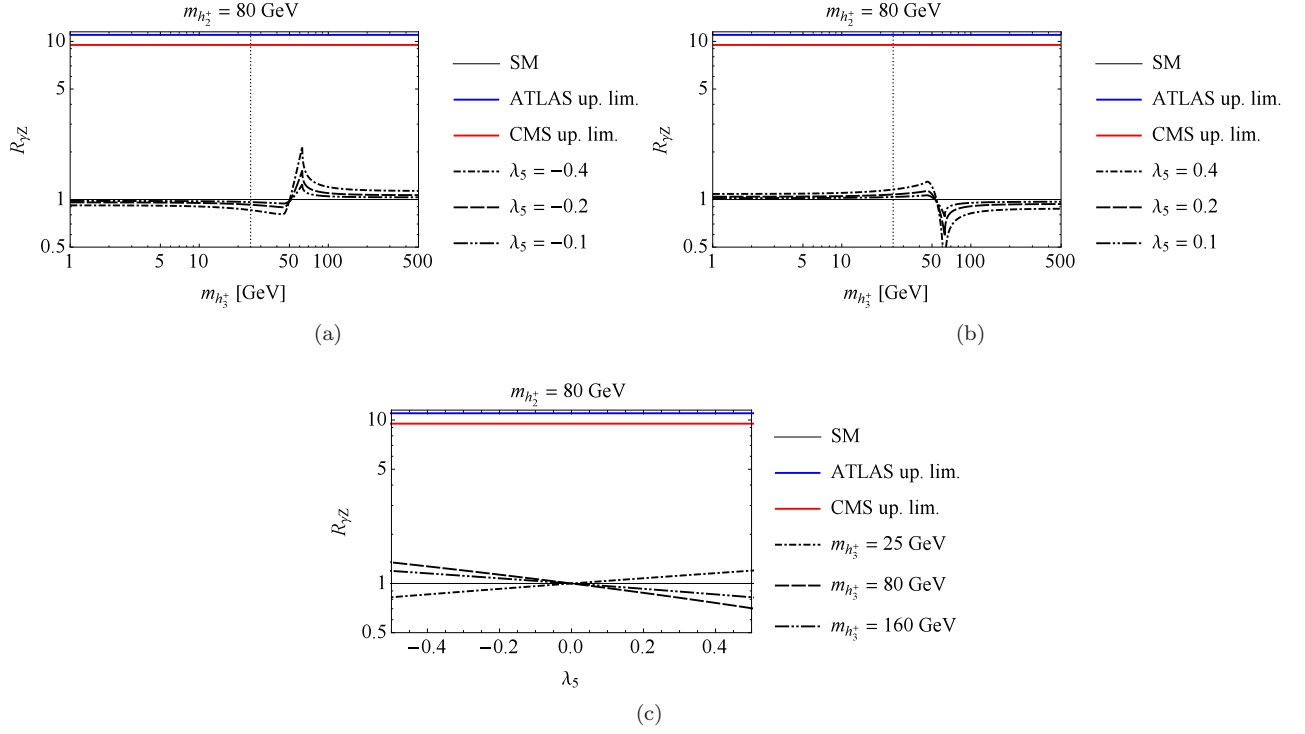


FIG. 4: $R_{\gamma Z}$ for $m_{h_2^+} = 80$ GeV fixed. In (a) and (b) consider $R_{\gamma Z}$ as function of $1 \leq m_{h_3^+} \leq 500$ GeV, but in (a) λ_5 is negative and in (b) is positive. In (c) $R_{\gamma Z}$ is presented as function of $-0.5 \leq \lambda_5 \leq 0.5$ with different values of $m_{h_3^+}$.

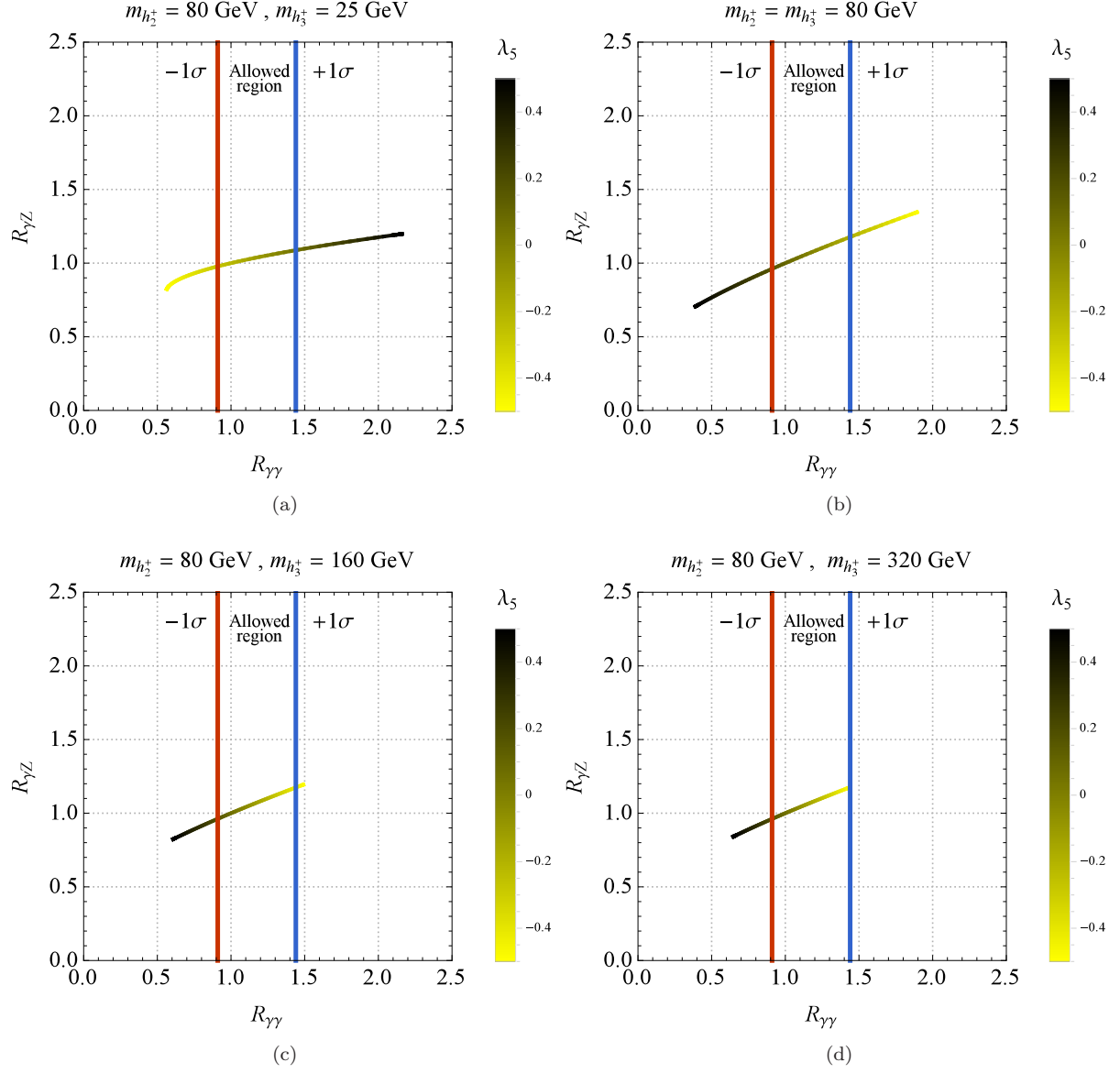


FIG. 5: Correlation between $R_{\gamma\gamma}$ and $R_{\gamma Z}$ as function of $-0.5 \leq \lambda_5 \leq 0.5$, with $m_{h_2^+} = 80 \text{ GeV}$ and various values of $m_{h_3^+}$.

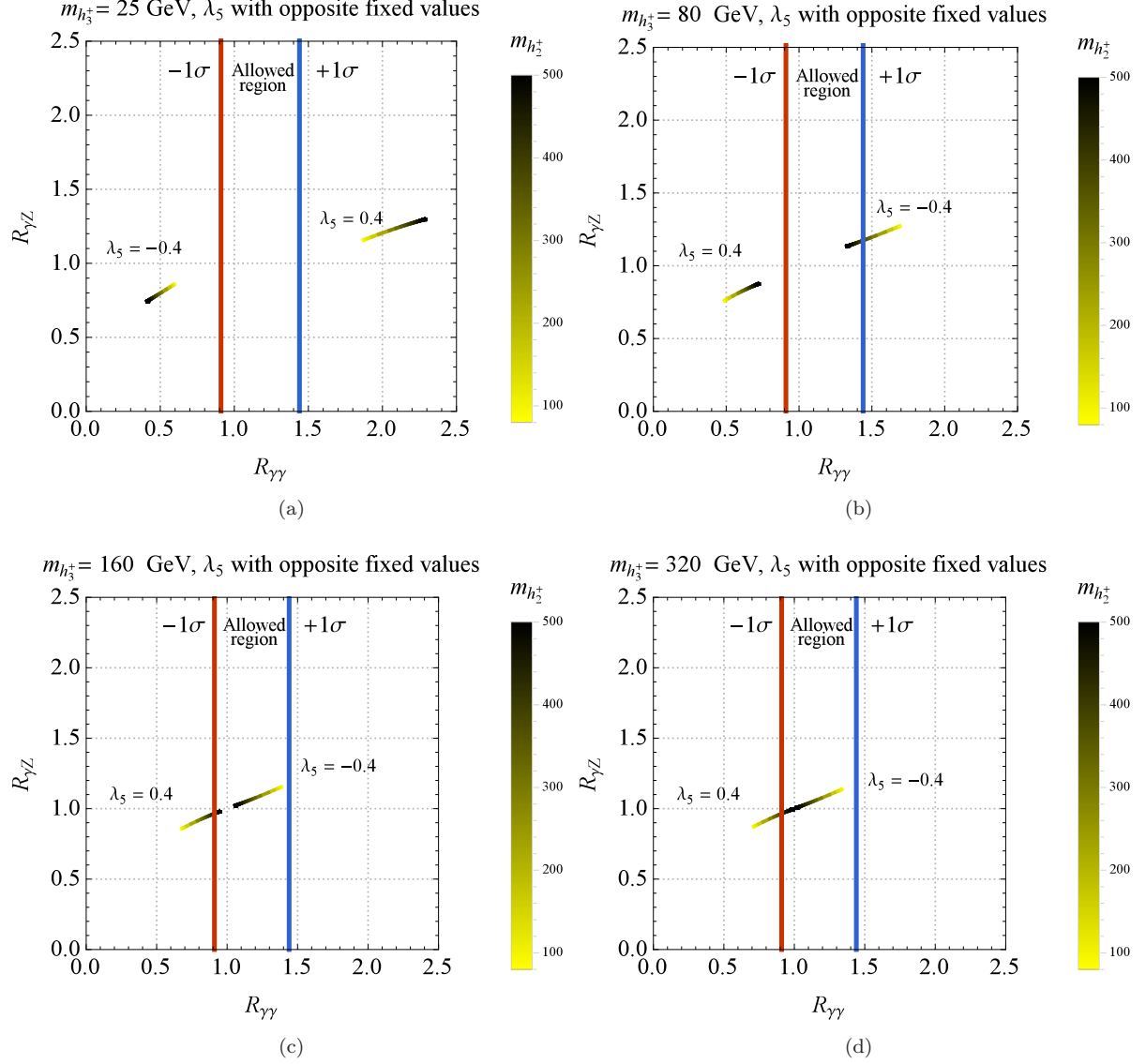


FIG. 6: Correlation between $R_{\gamma\gamma}$ and $R_{\gamma Z}$ as function of $m_{h_2^+}$, in the range $80 \text{ GeV} \leq m_{h_2^+} \leq 500 \text{ GeV}$, with $\lambda_5 = \pm 0.4$ and different cases of $m_{h_3^+}$.

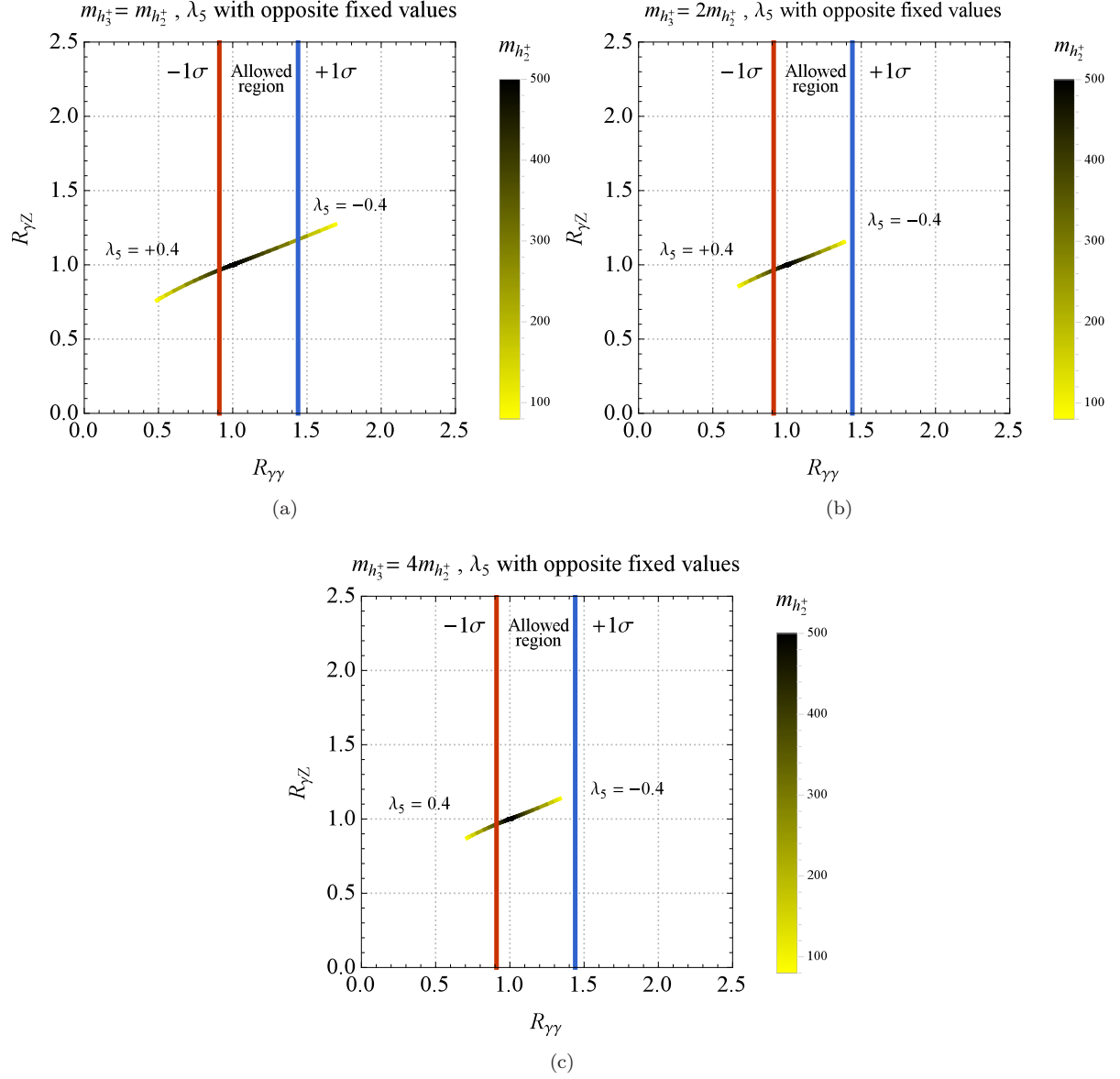


FIG. 7: Correlation between $R_{\gamma\gamma}$ and $R_{\gamma Z}$ as function of $m_{h_2^+}$, in the range $80 \text{ GeV} \leq m_{h_2^+} \leq 500 \text{ GeV}$, in cases where $m_{h_2^+} \propto m_{h_3^+}$, with $\lambda_5 = \pm 0.4$.

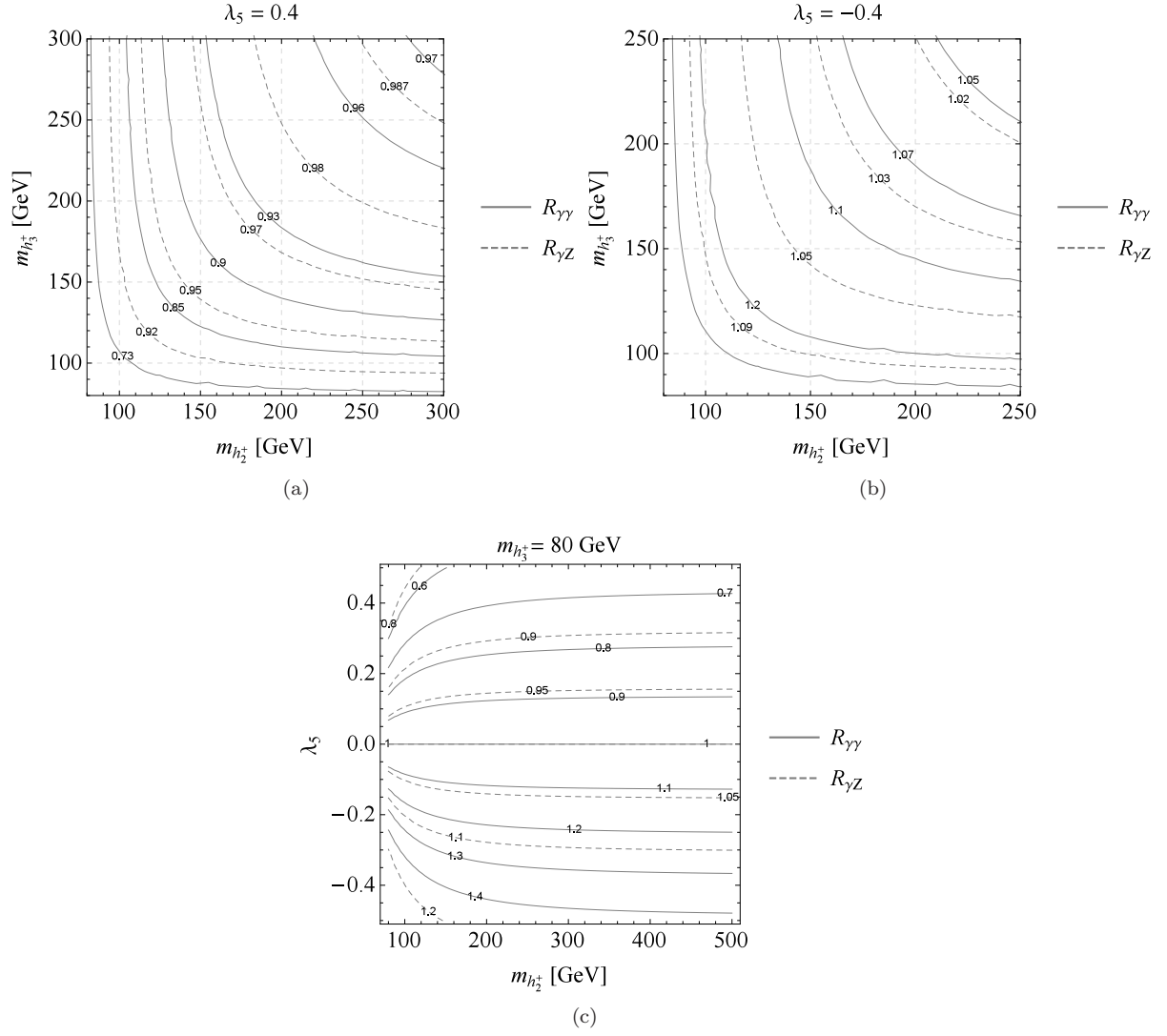


FIG. 8: $R_{\gamma\gamma}$ and $R_{\gamma Z}$, in (a) and (b) as function of $m_{h_{2,3}^+} \geq 80$ GeV with $\lambda_5 = \pm 0.4$, and in (c) as function of $m_{h_2^+} \geq 80$, $-0.4 \leq \lambda_5 \leq 0.4$ with $m_{h_3^+} = 80$ GeV.